ORIGINAL PAPER

A budget analysis of a long-lived tropical mesoscale vortex over Hainan in October 2010

Fu Shenming · Li Wanli · Sun Jianhua · Xia Rudi

Abstract The vorticity, eddy kinetic energy, and helicity budgets were calculated to study the variations of a long-lived tropical mesoscale vortex that occurred over Hainan during the period 05–09 October 2010. The main results are as follows: the vortex was mainly located at middle to lower levels of the troposphere, and among different levels, the dominant factors responsible for the variations of the vortex were different. Intense convergence at the lower troposphere dominated the formation and longevity of the vortex. The vertical transport of positive vorticity which was closely related to the convective activities was conducive to the formation and maintenance of the vortex. The barotropic energy conversion was favorable for the formation of the vortex, while the baroclinic energy conversion accelerated its attenuation. Background circulations were favorable for the longevity of the vortex, and interactions with other synoptic systems were important to its variations. The variation of helicity was closely related to the vortex, and the maintenance of positive helicity was another favorable factor for the longevity of the vortex.

F. Shenming (✉)
International Center for Climate and Environment Sciences,
Institute of Atmospheric Physics, Chinese Academy of Sciences,
Beijing 100029, China
e-mail: fusm@mail.iap.ac.cn

F. Shenming · X. Rudi
State Key Laboratory of Severe Weather,
Chinese Academy of Meteorological Sciences,
Beijing 100081, China

L. Wanli
Key Laboratory of Middle Atmospheric and Global Environment
Observation, Institute of Atmospheric Physics,
Chinese Academy of Sciences, Beijing 100029, China

S. Jianhua
Laboratory of Cloud-Precipitation Physics and Severe Storms,
Institute of Atmospheric Physics, Chinese Academy of Sciences,
Beijing 100029, China

1 Introduction

Mesoscale vortices are often associated with heavy rainfall and other severe weather phenomena (Tao 1980; Johnston 1982; Akiyama 1984; Bartels and Maddox 1991; Ninomiya 2000; Zhang and Ban 1996; Simpson et al. 1997; Tirer and Davis 2002; Knievel and Johnson 2002; Hendricks et al. 2004; Zhao et al. 2004; Shen et al. 2005; Zhou and Wang 2005; Montgomery et al. 2006; Ni and Zhou 2006; Fu et al. 2009; Fu et al. 2011b). Thus, mesoscale vortices have attracted research interests for years. Chen and Lorenzo (1984) simulated a mesoscale vortex over the East Asian monsoon region and found that under the coupling condition of the lower-level jet (LLJ) and upper-level jet (ULJ), the vortex could cause heavy rainfalls. Knievel and Johnson (2002) used the spatial bandpass filter to study a mesoscale vortex and found that the deepening of the vortex appeared to be reflected in the vertical wind shear at the vortex center. Using the high-resolution model simulations, Lu et al. (2002) analyzed the meso-β scale vortex in the mei-yu front and found that the development of mesoscale vortex system was closely related to the meso-scale transport and intense vertical motion in regional area under the moist neutral stratification condition. Zhao et al. (2004) studied the mechanism of heavy rainfalls over the mei-yu front in the Yangtze River basin and found that mesoscale vortices were the main influencing systems. Hendricks et al. (2004) found that at near-cloud-resolving scales, vortical hot towers were the preferred mode of

convection, and that the mesoscale vortex was favorable for the formation of tropical cyclone. Kirk (2007) used a phase-plot method to analyze the effects of different factors such as advections and latent heat release on the development of mesoscale vortex and found that latent heat release was very important for some vortices. Davis and Galarneau (2009) investigated the vertical structure of two cases of developing mesoscale vortices and found that the lateral transport of vorticity from the convective region back beneath the mid-tropospheric vorticity center was very important for the development of a deep column of cyclonic vorticity. Fu et al. (2009) calculated the budget of the eddy kinetic energy (EKE) of a mesoscale vortex and found that the background circulations could influence the formation and development of the vortex remarkably through transports.

During the early October 2010, Hainan experienced several heavy rainfall events, which caused floods affecting 16 cities and counties. The duration of the heavy rainfall episodes is longest since 1961. During the period of 0600 UTC 05 October–1800 UTC 09 October, a mesoscale vortex maintained over Hainan (HNV) and caused several heavy rainfall episodes with the maximum 3-h precipitation of up to 70 mm. The HNV lasted for approximately 108 h which is rare for mesoscale vortices, and the longevity of HNV was very favorable for the persistence of the heavy rainfall episodes.

In this paper, we focus on the HNV and try to answer the following three scientific questions: (a) which factors dominated the formation and dissipation of the HNV? (b) Why did the HNV last so long? (c) During the lifetime of HNV, what is the relationship between the HNV and background circulations? Data and methodology are discussed in Sect. 2. The evolution of the HNV and its associated heavy rainfall events are analyzed in Sect. 3, and the budget analyses of vorticity, EKE, and helicity are shown in Sect. 4. Summary and conclusions are given in Sect. 5.

2 Data and method

Final analysis data (four times daily) with horizontal resolution of $1° \times 1°$ from the National Centers for Environmental Prediction (NCEP) are used for calculation and analysis in this paper.[1] Conventional surface observations from the Korea Meteorological Administration (KMA), 3-h-precipitation from CMORPH with the resolution of 0.25°, eight times daily (Joyce et al. 2004), as well as hourly TBB (temperature of black body) data from the Satellite Fengyun (FY)-2E with a horizontal resolution of

0.1° × 0.1° are used to investigate the evolution of HNV, and the associated convective activities.

To explore answers to the three scientific questions raised in the introduction, three diagnostic tools are used, namely, the vertical vorticity budget equation, the EKE budget equation, and the vertical helicity budget equation.

2.1 The vertical vorticity budget equation

Since the vertical vorticity is an effective measurement of vortices, in this paper, we use the vertical vorticity budget equation from Kirk (2007) as Eq. 1 shown, to analyze the evolution of HNV:

$$\frac{\partial \zeta}{\partial t} = -\vec{V}_h \cdot \nabla_h \zeta \quad -\omega \frac{\partial \zeta}{\partial p} + \vec{k} \cdot \left(\frac{\partial \vec{V}_h}{\partial p} \times \nabla_h \omega \right) - \beta v - (\zeta + f) \nabla_h \cdot \vec{V}$$

$$\quad \text{V1} \qquad \text{V2} \qquad \text{V3} \qquad \text{V4} \qquad \text{V5}$$

$$\tag{1}$$

where ζ is the vertical component of vorticity; $\vec{V}_h = u\vec{i} + v\vec{j}$ is the horizontal velocity vector, and $\vec{i}, \vec{j}, \vec{k}$ stand for the unit vector points to the east, north as well as zenith, respectively; $\nabla_h = \frac{\partial}{\partial x}\vec{i} + \frac{\partial}{\partial y}\vec{j}$ is the horizontal gradient operator; $f = 2\Omega \sin\varphi$ is the Coriolis parameter, Ω is the rotational angular velocity of the earth, φ is the latitude; p is the pressure; $\omega = \frac{dp}{dt}$; and $\beta = \frac{\partial f}{\partial y}$.

Term V1 stands for the horizontal advection of vertical vorticity; term V2 is the vertical advection of vertical vorticity; term V3 reflects the influences of titling, namely the conversion between the horizontal and vertical vorticity (Davis and Galarneau 2009); term V4 represents the "β effect" which is related to the geographical position; and term V5 reflects influences associated with the divergence.

2.2 The EKE budget equation

The HNV is not an isolated system; background circulations are important to its longevity. In order to investigate the interactions between the HNV and background circulations, the budget equation of EKE is employed (Ding and Liu 1985; Fu et al. 2009) as shown in Eq. 2:

$$\frac{\delta \overline{[K_E]}}{\delta t} = I(K_Z, K_E) + I(P_E, K_E) + F_H(K_E) + F_V(K_E) + F_H(P_E) + F_V(P_E)$$

$$\quad \text{K1} \qquad \text{K2} \qquad \text{K3} \qquad \text{K4} \qquad \text{K5} \qquad \text{K6}$$

$$\tag{2}$$

The left-hand side of Eq. 2 is the local variation of the area-averaged EKE, and the right-hand side terms are defined as K1–K6. Terms are discussed as follows:

---

[1] Compared with the horizontal range and time span of the vortex in our case, the NCEP data is enough to resolve the vortex. Moreover, our calculation also indicate that the NCEP data can capture the main characteristics of the vortex and guarantee the accuracy for a qualitative analysis.

$I(K_Z, K_E) = -\overline{[u'v']\frac{\cos\varphi}{a}\frac{\partial}{\partial\varphi}\frac{[u]}{\cos\varphi}} - \overline{[v'v']\frac{1}{a}\frac{\partial[v]}{\partial\varphi}} - \overline{[u'\omega']\frac{\partial[u]}{\partial p}}$
$-\overline{[v'\omega']\frac{\partial[v]}{\partial p}} + \overline{[u'u'][v]\frac{\tan\varphi}{a}}$ is defined as K1, which represents the transition between zonal mean kinetic energy and EKE, namely the barotropic energy conversion. $I(P_E, K_E) = -\frac{R}{p}\overline{[\omega'T']}$ is defined as K2, which represents the transition between available potential energy and EKE, i.e. the baroclinic energy conversion. $F_H(K_E) = -\overline{[\frac{1}{a\cos\varphi}\frac{\partial(uK_E)}{\partial\lambda}]} - \overline{[\frac{1}{a\cos\varphi}\frac{\partial(vK_E\cos\varphi)}{\partial\varphi}]}$ is defined as K3, which is the horizontal transport of EKE by background circulations. $F_V(K_E) = -\overline{[\frac{\partial(\omega K_E)}{\partial p}]}$ is defined as K4, which represents the vertical transport of EKE by background circulations. $F_H(P_E) = -\overline{[\frac{1}{a\cos\varphi}\frac{\partial(u'\phi')}{\partial\lambda}]} - \overline{[\frac{1}{a\cos\varphi}\frac{\partial(v'\phi'\cos\varphi)}{\partial\varphi}]}$ is defined as K5, which represents the horizontal transport of eddy geopotential energy by horizontal wind perturbations. $F_V(P_E) = -\overline{[\frac{\partial(\omega'\phi')}{\partial p}]}$ is defined as K6, which represents the vertical eddy flux of eddy geopotential energy by the vertical wind perturbation. It should be noted that terms K5 and K6 could reflect the effects from other synoptic systems. In the aforementioned definitions, [ ] stands for zonal mean (in this paper, it is calculated from 70°E to 150°E); thus variables can be written as $p = [p] + p$, where p' represents eddy. $\overline{[p]}$ stands for area-averaged variable. λ is longitude; a the radius of the earth; R the gas constant; ϕ the geopotential; $K_E = \frac{1}{2}(u'^2 + v'^2)$ the EKE per the unit mass, and $K_Z = \frac{1}{2}([u]^2 + [v]^2)$ the area-averaged zonal mean kinetic energy.

2.3 The vertical helicity budget equation

Lilly ([1986]) indicates that, besides the use for illustrating structures of rotating storms, helicity also suggests the existence of fundamental differences of behavior between storms with and without strong rotation. Furthermore, he found that helicity effects seemed to be dominant in long-lived storms, since helicity could reduce the energy loss due to dissipation. In this paper, the vertical helicity budget equation shown as Eq. [3] (Fu et al. [2011a]) is employed to calculate the budgets of helicity which is closely related to the longevity of HNV.

$$\frac{dh_z}{dt} = -\zeta_z\left(\frac{1}{\rho}\frac{\partial p}{\partial z} + g\right) - w\xi_z - \beta vw - w(\zeta_z + f)(\nabla_h \cdot \vec{V}_h) + \vec{\zeta}_h \cdot \nabla_h K_z$$

$$\qquad\quad \text{Z1} \qquad\quad \text{Z2}\quad \text{Z3} \qquad\quad \text{Z4} \qquad\quad\quad \text{CON}$$
$$(3)$$

where $h_z = w\zeta_z$ [2] is the vertical helicity, $w = dz/dt$, ρ is the density, g is the acceleration due to gravity, ξ_z is the vertical solenoid, and $\vec{\zeta}_h$ is the horizontal component of vorticity vector $\vec{\zeta} = \nabla \times \vec{V}$, where $\nabla = \frac{\partial}{\partial x}\vec{i} + \frac{\partial}{\partial y}\vec{j} + \frac{\partial}{\partial z}\vec{k}$, and $K_z = \frac{1}{2}w$ is the vertical kinetic energy.

Term Z1 is caused by vertical acceleration which is closely associated with the buoyancy; Z2 is caused by the vertical solenoid which is closely related to the baroclinity of the atmosphere; Z3 is related to the "β effect" which reflects the influences of geographical position; Z4 indicates the effects from divergence; and CON reflects the conversion between vertical and horizontal helicity (Fu et al. [2011a]).

3 Weather discussions

At 0000 UTC 05 October 2010, the mainland of China was dominated by a high-pressure system (Fig. [1]a). At the same time, there was a low stretching from the Bay of Bengal to Hainan, with a low-pressure center of 1,005 hPa formed near Hainan. Twelve hours later, the high-pressure system weakened, while the wind associated with the low-pressure center enhanced up to 15 m s^{-1} approximately (not shown). Thus, the low-pressure center intensified into a tropical depression (TD). Then the TD lasted for nearly 120 h as Fig. [1]b–d shown, and dissipated at 1200 UTC 10 October 2010. It is worth noting that, from 0000 UTC 07 October 2010, the low-pressure system stretching from the Bay of Bengal enlarged eastward with time (Fig. [1]c, d). However, during this period, the high-pressure system shrank and moved east.

The stream field of 850 hPa at 0000 UTC 05 October show a vortex over the Indo-China Peninsula (Fig. [2]a). To the northeast of the vortex, there was a strong shear zone with intense positive vorticity, ascending motions (Fig. [2]a), and convective instability (not shown). Below 650 hPa, there were intense cold and warm advections associated with the north and south wind, respectively (not shown), within the shear zone, which were favorable for enhancement of convective activities. Six hours later, the HNV which was associated with the low-pressure center at the surface (Fig. [1]) formed over Hainan. As a result, the positive vorticity, ascending motion, cold and warm advections all enhanced (not shown) within the dashed rectangles (16°–22°N, 106°–113°E), which is specified as the key area (KA) of the HNV.

---

[2] The vertical helicity reflects the flow point moves along the direction of the vertical vorticity vector. Therefore, it is an efficient measurement of both the vertical motion and rotation of the vortex.
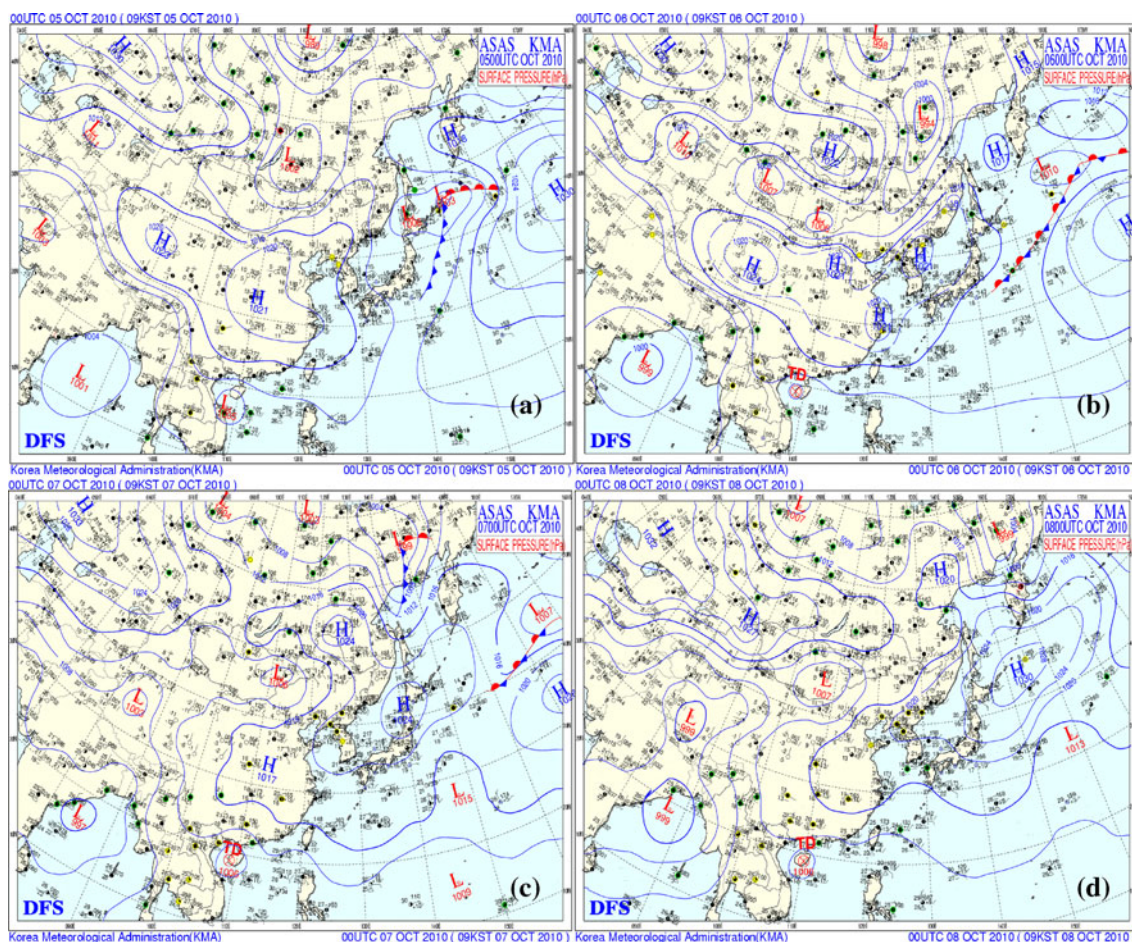
Fig. 1 Surface observation charts from the Korea Meteorological Administration (KMA), where **a** is 0000 UTC 05 October 2010, **b** is 0000 UTC 06 October 2010, **c** is 0000 UTC 07 October 2010, and **d** is 0000 UTC 08 October 2010

The HNV remained quasi-stationary within the dashed rectangles (Fig. 2) for 108 h approximately, and it dissipated at 0000 UTC 10 October. From the vertical stretching (Fig. 2g) of HNV, during its lifetime, HNV was mainly located at middle to lower levels of the troposphere (500 hPa and below). The intense warm and cold advection centers as well as convective instable areas were also mainly located below 500 hPa (not shown). For the duration of the HNV, intense ascending motions mainly occurred in warm advection areas, and positive temperature deviation centers (the maximum temperature deviation is above 2 °C) closely associated with latent heat release appeared among levels of 700–300 hPa (not shown). As Fig. 2d depicted, from 0000 UTC 08 October, the HNV weakened significantly. Meanwhile, the ascending motion, meridional wind, and temperature advections associated with the HNV also weakened (not shown). Therefore, the period of 0600 UTC 05 October–0000 UTC 08 October is defined as the maintaining stage (MS) of HNV, and the period of 0000 UTC 08 October–1800 UTC 09 October as the decaying stage (DS).

As depicted in Fig. 3a, 6-h before the formation of HNV, there was a low zone stretching from the Bay of Bengal to Hainan at 500 hPa, corresponding to the low-pressure zones at the surface (Fig. 1a). The ULJ at 200 hPa was located around 30°N, and the LLJ at 700 hPa appeared around the low center over the Indo-China Peninsula. Six hours later, when the HNV formed, a low center of 5,850 gpm appeared over Hainan, while the ULJ and LLJ both weakened (not shown). During the MS, the low center and LLJ over Hainan weakened and then disappeared (Fig. 3b). The ULJ moved southward to 27°N approximately, and the subtropical high remained quasi-stationary with its west boundary around 113°E (Fig. 3b), which was possibly favorable for the stability of the HNV. During the DS, the ULJ weakened and moved northward (Fig. 3c), while the LLJ enhanced significantly near 27°N corresponding to the intense horizontal shear there. The subtropical high weakened significantly at 0000 UTC 09 October (Fig. 3c) and when the HNV dissipated (Fig. 3d; 0000 UTC 10 October), the subtropical high re-enhanced with high-pressure zones appearing over Hainan.
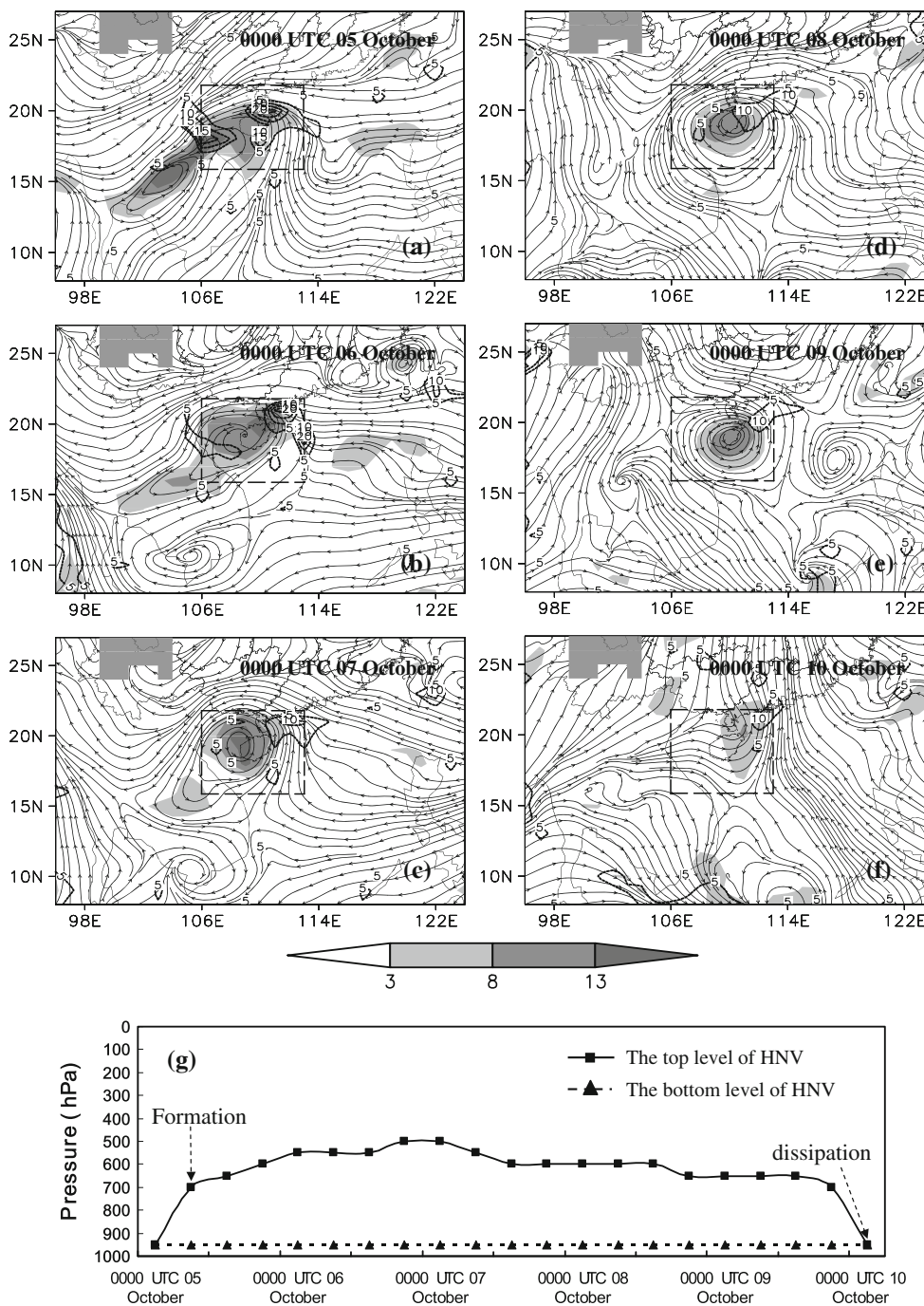
Fig. 2 a–f Stream field at 850 hPa, where the shaded is vorticity (10^{-5} s^{-1}), the *dashed rectangle* is the key area of vortex, *dashed* line denotes vertical velocity (10^{-2} m s^{-1}), and topography higher than 1,500 m is shaded in *gray*. **g** Vertical stretching levels during the life time of HNV

As shown in Fig. 4, heavy rainfall events occurred before the formation of the HNV. When the HNV formed, rains remained intense, with two maximum centers of 50 mm around Hainan (not shown). At 0000 UTC 06 October, the rainfall weakened (Fig. 4), and it re-enhanced from 0900 UTC 06 October. The heavy rainfall mainly occurred in the central, south, and east parts of the HNV (Fig. 4), where there were very intense ascending motions

(Fig. 2), and the precipitation rate during the MS was more than that of the DS.

Figure 5 shows the convective activities during the lifetime of HNV. Intense convective activities occurred mainly at the center, south, and east of the HNV, where there were intense ascending motions (Fig. 2) and enough moisture supply (not shown). The minimum of TBB was below −72°C (Fig. 5), which indicates that the convection
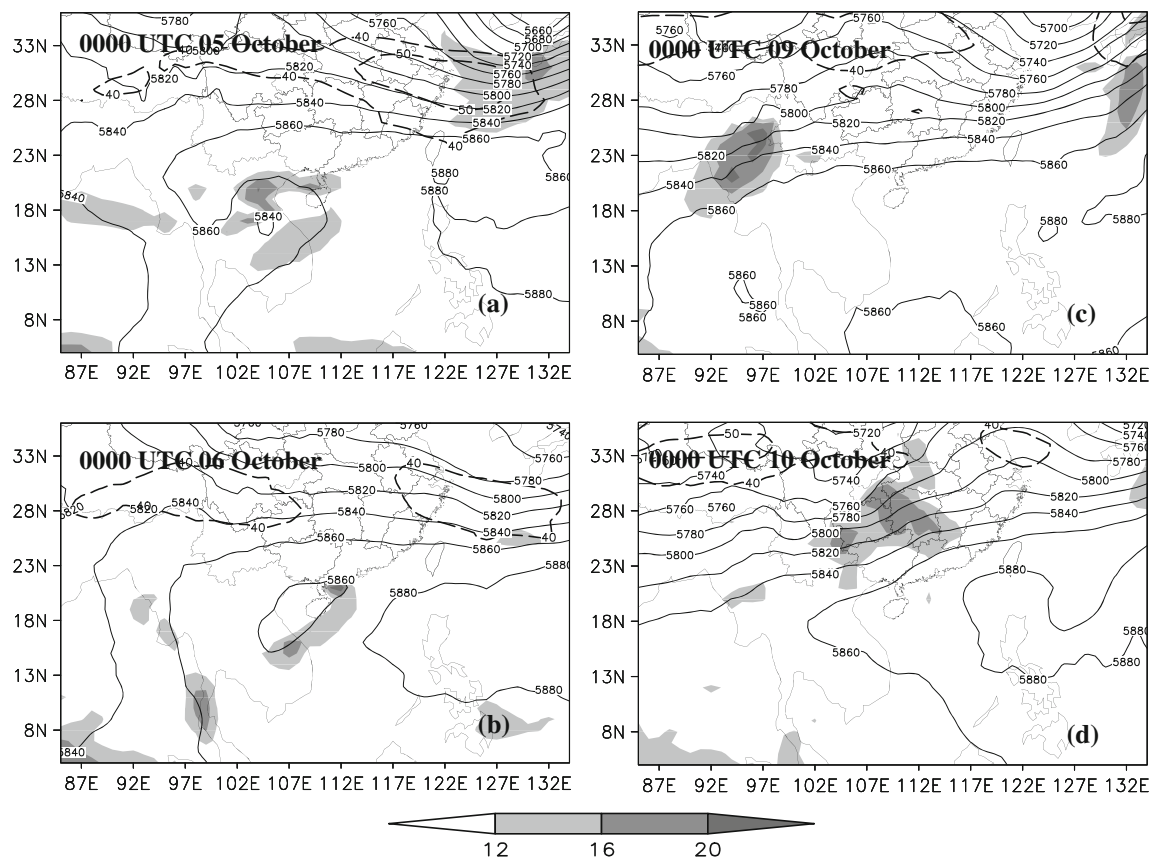
Fig. 3 Distribution of geopotential height at 500 hPa (*solid*; m), high-level-jet at 200 hPa (*dashed*; m s^{-1}), and low-level-jet at 700 hPa (*shaded*; m s^{-1})

was very intense (up to 100 hPa). During the period of MS, TBB varied significantly, and at 0600 UTC 06 October, convection was weakest (not shown), which maybe caused by the reduction of moisture supply (not shown). During the period of DS, convective activities remained intense and were mainly located in the southeast of the HNV. It should be noted that the spatial pattern of the rainfall is consistent with the convective activities well (Figs. 4, 5), and they both moved east. Thus, during the lifetime of HNV, the activities of the easterly wave[3] was not obvious (Arnault and Roux 2010), and therefore, the HNV is different from the vortices associated with the easterly wave.

4 Diagnosis of the HNV

Three diagnostic tools were employed to solve the scientific questions listed in the introduction: (a) the budget of vorticity was used to analyze factors associated with the evolution of the HNV; (b) the budget of EKE was employed to investigate

the energy characteristics of the HNV as well as the interactions between the HNV and background circulations; and (c) the budget of helicity was used to analyze the variation of helicity, which could resist the loss of energy, and thereby is very favorable for the longevity of the HNV.

4.1 Budgets of vorticity

Figure 6 depicts the vertical cross sections of key-area-averaged budgets of the vorticity equation. Within the KA, ascending motions dominated the whole life cycle of the HNV (Fig. 6a). Intense ascending motions mainly remained during the MS, especially the initiation period of HNV, which may be related to the intense divergence at high levels of the troposphere (HT). During the MS, descending motions were weak and only appeared at HT, while during the DS, descending motions enhanced significantly and mainly located at the middle to lower levels of the troposphere (MLT). Positive vorticity was mainly located at the MLT with negative vorticity aloft, and the depth of positive vorticity layers reduced with time, which was consistent with the variations of vertical stretching of the HNV approximately (Fig. 2g). Convergence mainly remained at lower levels of the troposphere (LT), with

---

[3] The convective activities associated with the easterly wave always move westward, and the inverted "V" cloud systems can often be found in the easterly wave.
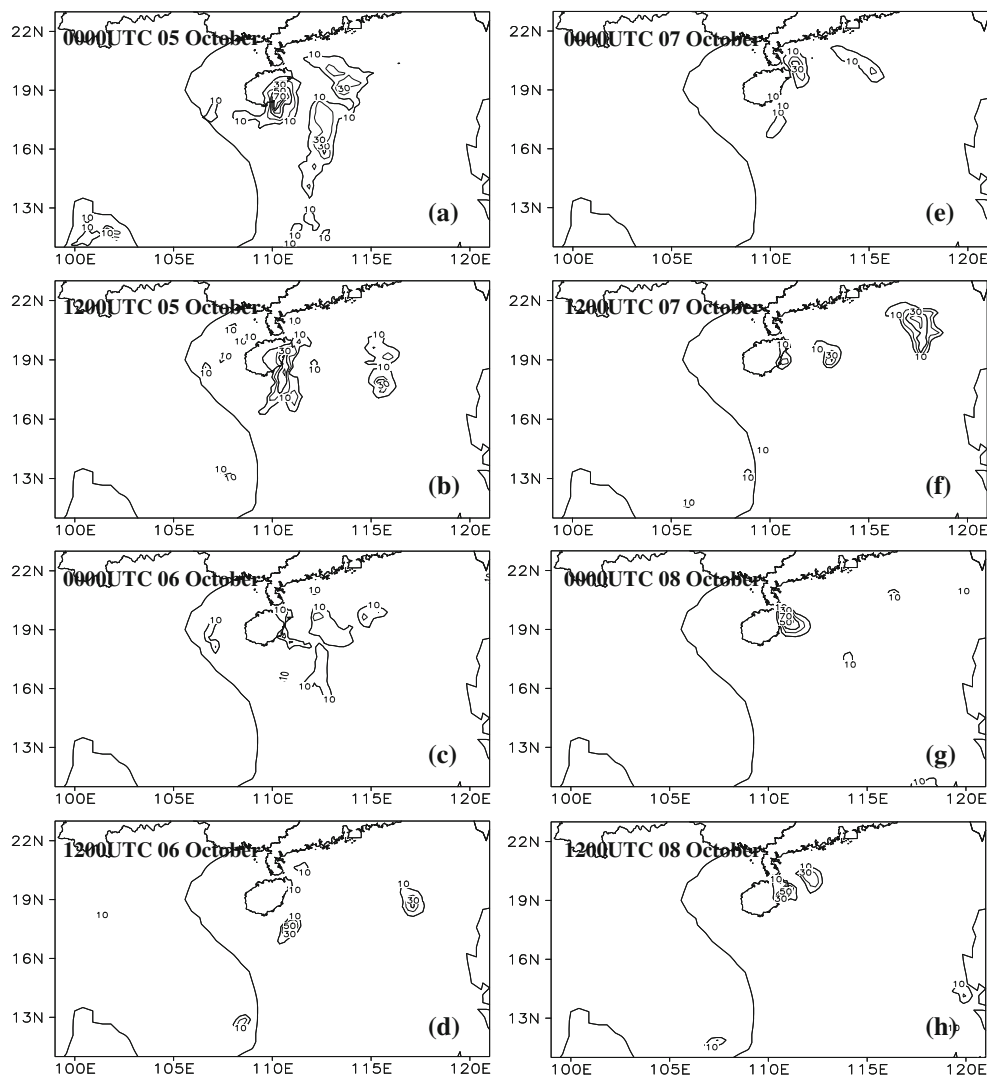
Fig. 4 Three-hour-precipitation from CMORPH (mm) with the resolution of 0.25°, eight times a day

weak divergence located at middle levels of the troposphere (MT). Thus the configuration of convergence and divergence was favorable for the maintenance of ascending motions, while the depth of convergence layer also reduced with time. It should be noted that convergence weakened significantly at 0000 UTC 08 October, and the vorticity also weakened remarkably, both of which indicated that the HNV began decaying. During the DS, positive vorticity and convergence weakened with time; at 0000 10 October, when the HNV dissipated, convergence weakened remarkably at the LT while remaining intense at the middle to high levels of the troposphere, which was conducive to the enhancement of descending motions.

As Fig. 6b depicts, during the lifetime of HNV, the zero-isoline of horizontal advection of vorticity (term V1) divided the diagram into three parts: the negative advections dominated the LT, which transported positive vorticity out of the KA; the positive areas approximately forms

the shape of a triangle, with maximum centers appearing at the initiation period of the HNV, which were very favorable for the development of HNV, while the depth of the positive layer reduced with time; and above the positive areas, there were large negative areas, with intense negative centers remaining at the HT. Before the formation of HNV, the positive vertical advection of vorticity (term V2) associated with convective activities (Fig. 5a) was very intense among levels of 850–550 hPa, which was favorable for the formation of HNV. Then the vertical advection weakened and only remained weak positive throughout the levels of the HNV which was favorable for the maintenance of HNV. It should be noted that, around 0000 UTC 06 October, the negative vertical advection enhanced at the LT. After 0000 UTC 09 October, the negative vertical advection intensified at the high levels of the HNV (HLHNV), thereby accelerating the attenuation of the HNV. As shown in Fig. 6c, the tilting term (V3) mainly
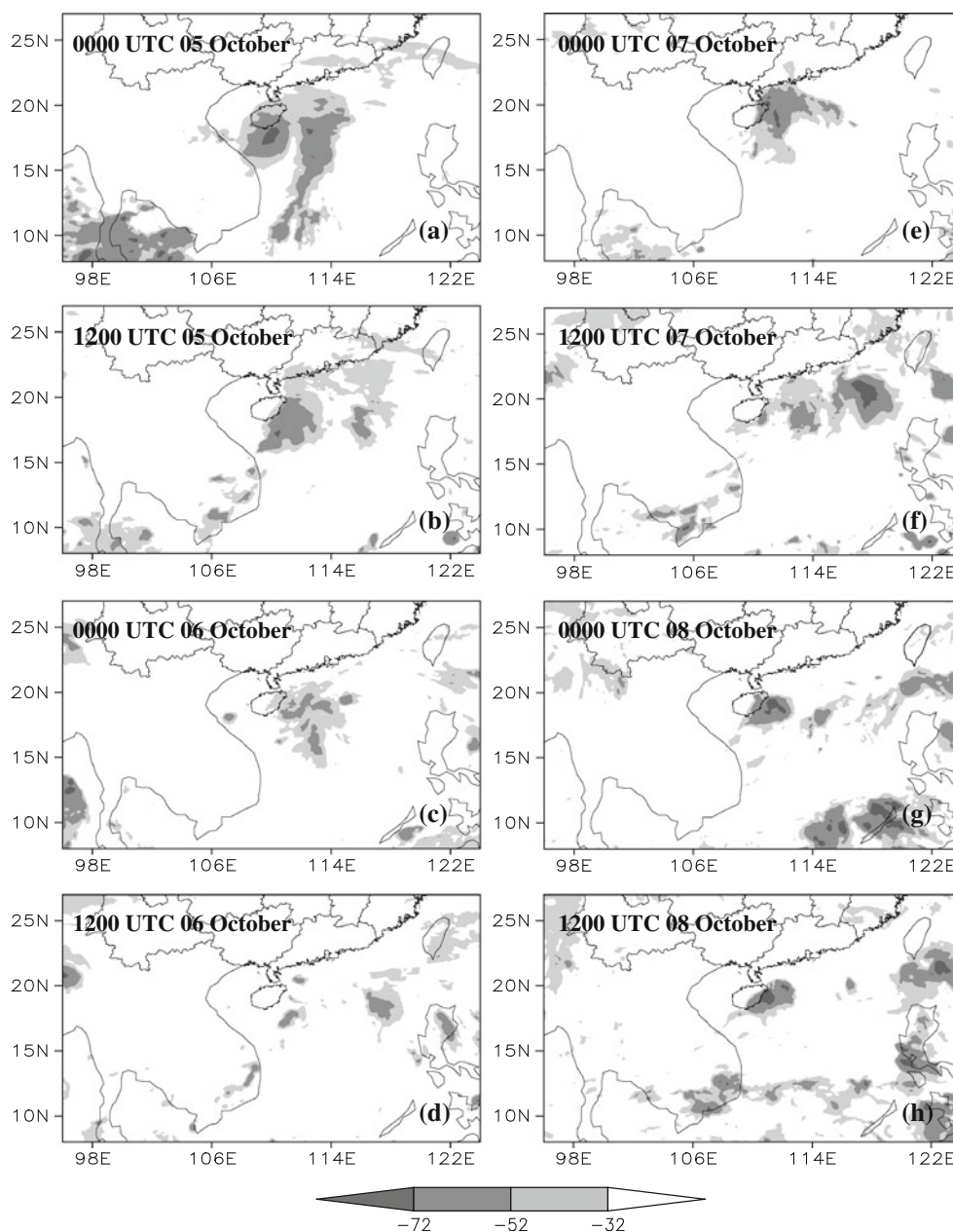
Fig. 5 TBB from Satellite FY-2E (°C)

converted the vertical vorticity into horizontal one which reduced the positive vorticity of HNV. However, during the initiation period of HNV, the tilting term was conducive to the enhancement of vorticity at the LT. It is worth noting that, around 0000 UTC 07 October, the tilting term also remained positive at the HLHNV, which was favorable for the maintenance of HNV. As Fig. 6d depicts, convergence (term V5) was favorable for the formation and maintenance of HNV at lower levels of the HNV (LLHNV), while divergence was conducive to the decaying of HNV at the HLHNV. Term V4 (β effect) only had slight effects on the

HNV, with negative effects dominating the MS and positive effects dominating the DS (Fig. 6e).

In order to identify the factors directly responsible for the formation and dissipation of the HNV, budgets of vorticity and EKE at 0000 UTC 05 October (6 h before the formation) and 1800 UTC 09 October (6 h before the dissipation) were scrutinized in detail. Six hours before the formation of HNV, there was a positive vorticity column stretching from 950–250 hPa (Fig. 7a). At the LT, convergence (term V5) was very favorable for the enhancement of vorticity, and below 850 hPa, tilting term (V3) was
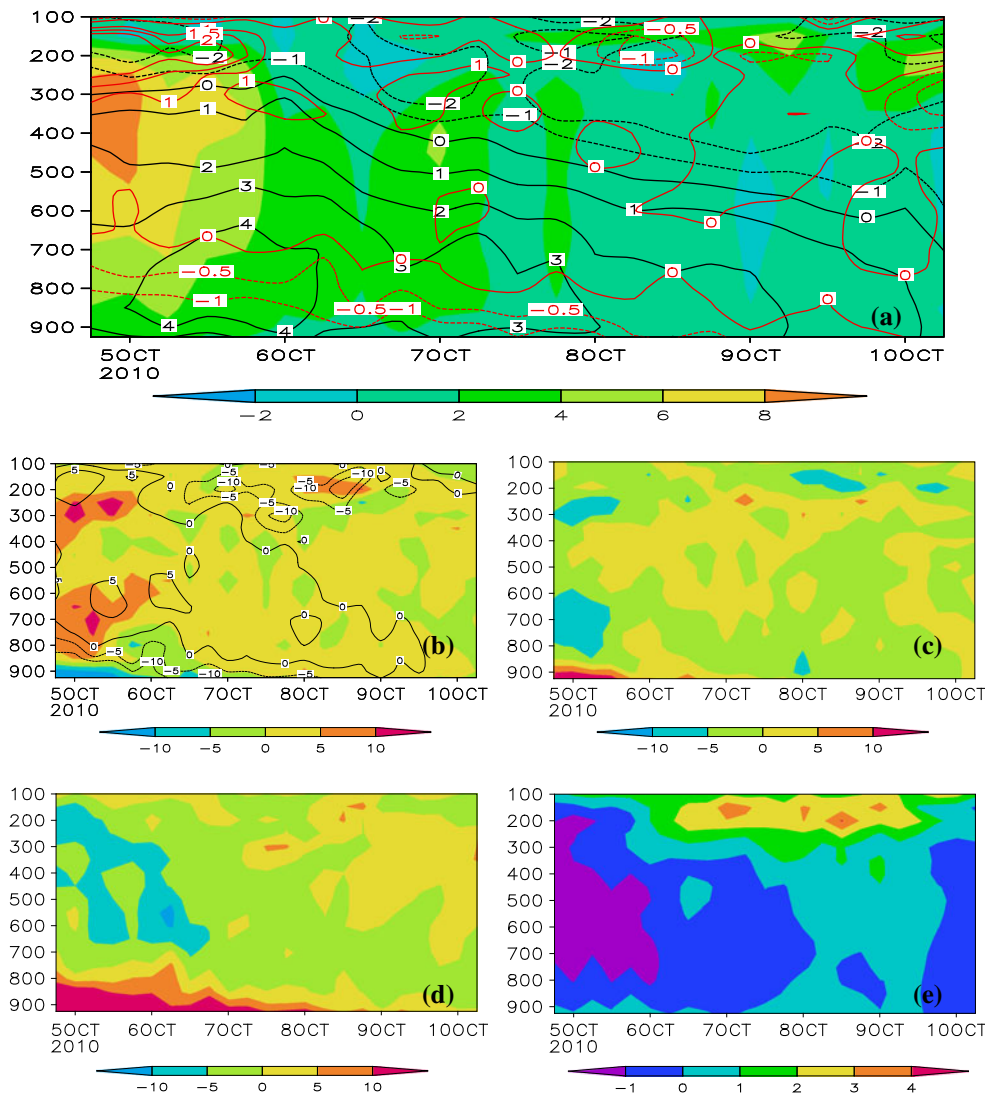
Fig. 6 Key-area-averaged budgets of vorticity: **a** is vorticity (*solid and dashed*; 10^{-5} s^{-1}), divergence (*solid and dashed*; 10^{-5} s^{-1}), and vertical velocity (*shaded*; 10^{-2} m s^{-1}); **b** Term V1 (*solid and dashed*; 10^{-10} s^{-1}) and term V2 (*shaded*; 10^{-10} s^{-1}); **c** Term V3 (10^{-10} s^{-1}); **d** Term V5 (10^{-10} s^{-1}); and **e** Term V4 (10^{-10} s^{-1})

also beneficial to the formation of HNV. From 850 to 500 hPa, the vertical advection of vorticity (V2) associated with the convective activity (Figs. 5a, 6a) was positive which contributed to the increase of vorticity. Weak positive horizontal advections (term V1) appeared around 700 hPa, and the β term (V4) remained slightly negative at the MLT. As a result, the convergence at the LLHNV and the vertical advections of vorticity at the HLHNV were dominant factors to the formation of HNV. From Fig. 7b, 6 h before the dissipation of HNV, the horizontal advection dominated the dissipation of HNV. It should be noted that the tilting term was also a very important factor which accelerated the dissipation of HNV at the LLHNV.

In order to identify the dominant factors during the MS and DS, the time average of the vorticity budgets were calculated as shown in Fig. 8. During the MS, the total

effect of V1–V5 remained positive (Fig. 8a) at all the levels of the HNV, which was favorable for the maintenance of HNV. At the LLHNV, convergence dominated the maintenance of HNV, and the tilting term was also favorable for maintaining the HNV, while at the HLHNV, horizontal and vertical advections were the most favorable factors for HNV. During the DS, the intensity of vorticity budgets weakened significantly (Fig. 8b), and the total effects of V1–V5 mainly became negative (except for levels below 850 hPa), which was corresponding to the attenuation of the HNV. The vertical advection and convergence were the most important factors which resisted the decaying of the HNV at the HLHNV and LLHNV, respectively, while the divergence and tilting terms dominated the decaying processes of the HNV at the HLHNV and LLHNV, respectively.
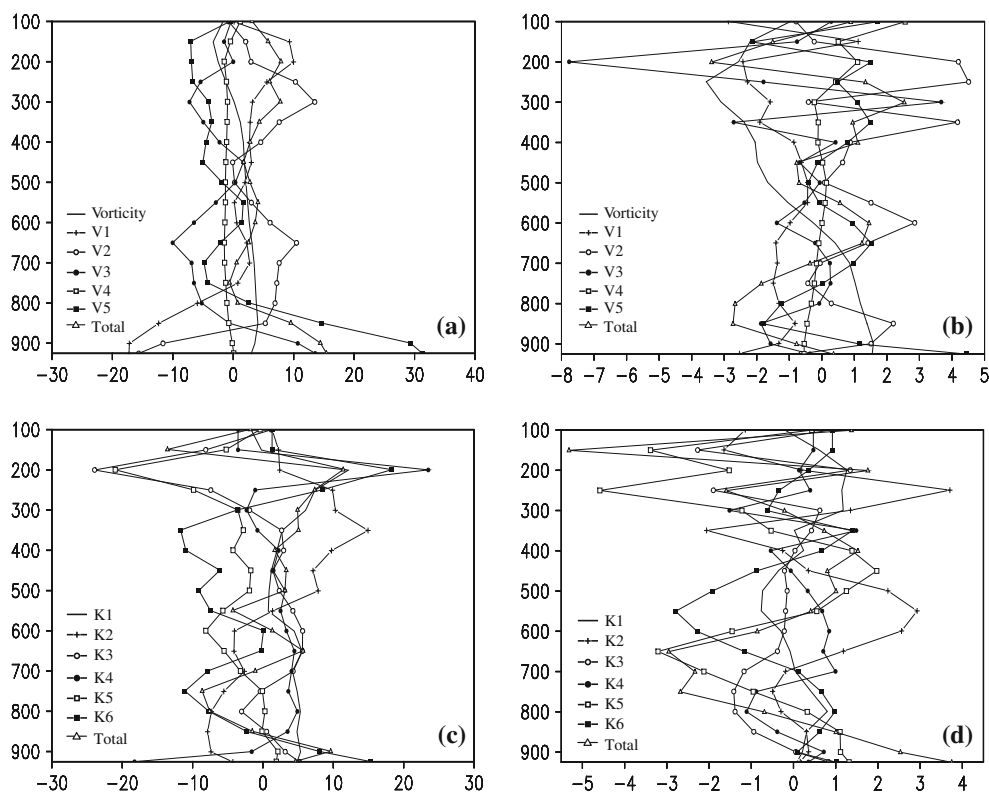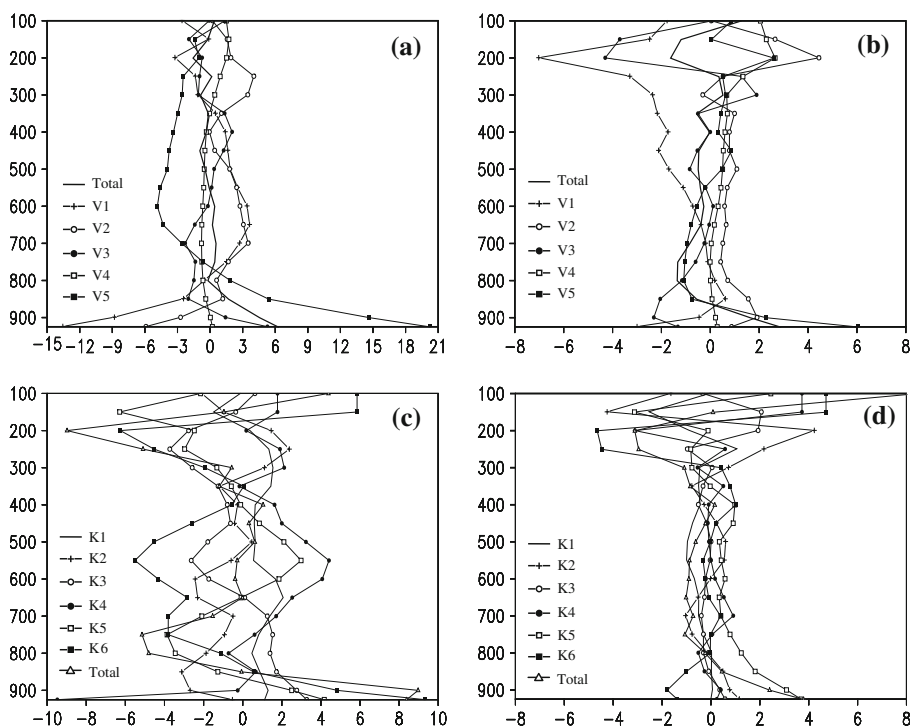
Fig. 7 Key-area-averaged budgets of vorticity and eddy kinetic energy. **a**, **b** Budgets of vorticity, where the unit of vorticity is $10^{-5}s^{-1}$, and units of terms V1–V5 and total are 10^{-10} s^{-2}. **c**,

d Budgets of EKE (10^{-4} J kg^{-1} s^{-1}). **a**, **c** At 0000 UTC 05 October 2010; **b**, **d** At 1800 UTC 09 October 2010

Fig. 8 Time average of key-area-averaged budgets of vorticity and eddy kinetic energy. **a**, **b** Budgets of vorticity (10^{-10} s^{-2}). **c**, **d** Budgets of EKE (10^{-4} J kg^{-1} s^{-1}). **a**, **c** Averaged during the MS; **b**, **d** Averaged during the DS
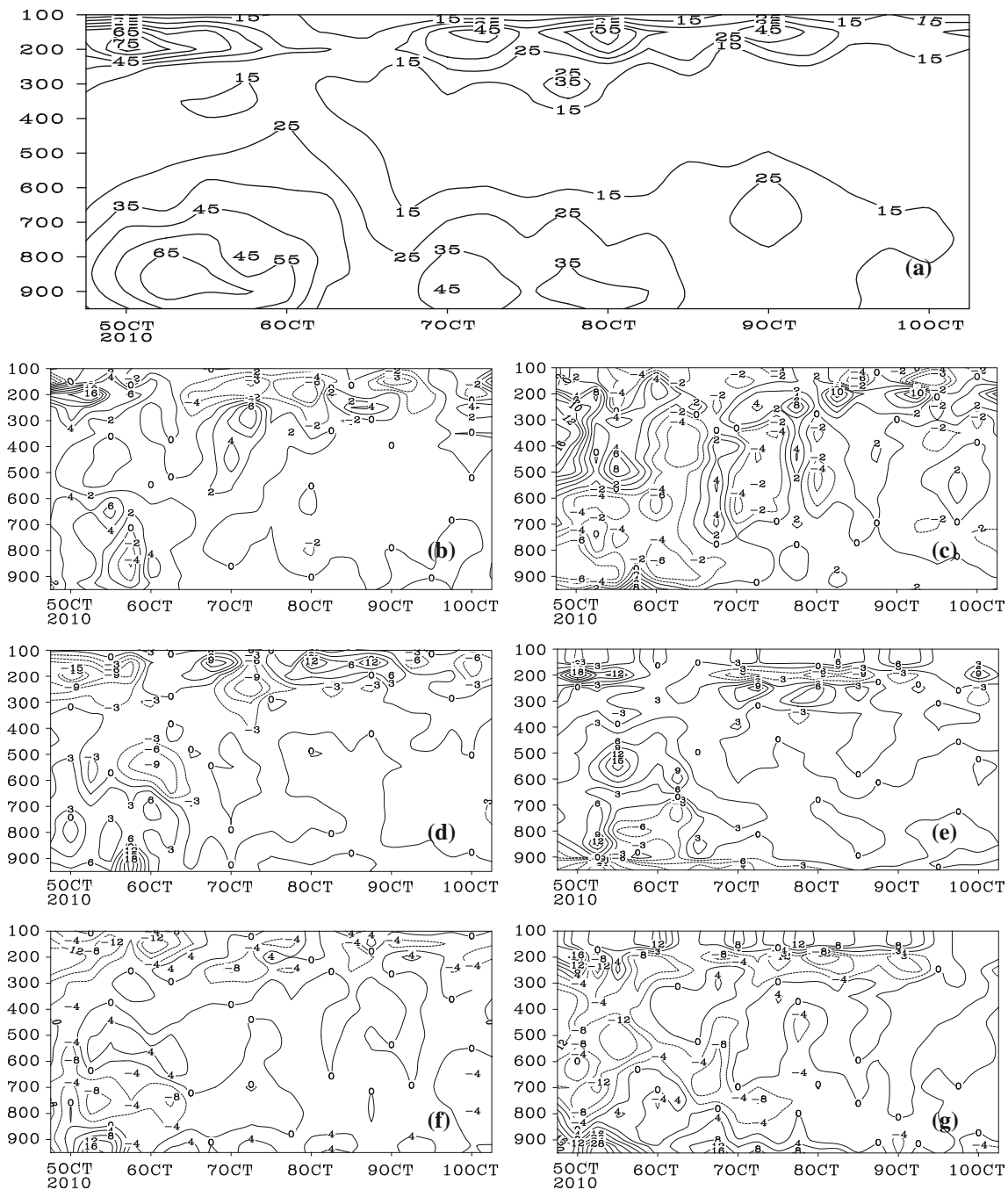
Fig. 9 Cross sections of key-area-averaged eddy kinetic energy and results of eddy kinetic energy budget equation, where **a** depicts the key-area-averaged EKE (J kg^{-1}); **b** term K1; **c** term K2; **d** term K3; **e** term K4; **f** term K5; and **g** term K6. The units of **b–g** is 10^{-4} J kg^{-1} s^{-1}

4.2 Budgets of EKE

There were two large EKE zones (Fig. 9a): one was at the HT, and the other was located at the MLT which was corresponding to the HNV. Comparing Fig. 9a with Fig. 6a reveals that the variation of the vorticity was approximately consistent with EKE, indicating that the wave shape was consistent with the wave energy well. Thus, there was no

remarkable frequency dispersion during the lifetime of HNV, and this was very conductive to the longevity of the HNV. During the MS, EKE remained very intense which was consistent with the maintenance of HNV. During the DS, the EKE decreased significantly, which was corresponding to the decaying process of the HNV. From Fig. 9b and c, during the lifetime of the HNV, the intensity of barotropic and baroclinic conversions differed from each

other slightly, and this indicates that the HNV is significantly different from the extratropical vortices, whose baroclinic conversions are more intense than the barotropical one (Fu et al. 2009). During the MS, especially the initiation stage of HNV, barotropic energy conversion (term K1) was mainly favorable for the development of HNV (Fig. 9b). Then in the DS, the barotropic energy conversion weakened significantly, with positive areas only remaining at the LLHNV. In the MS, the baroclinic conversion (term K2) mainly served as a sink for the HNV (Fig. 9c), whereas during the DS, it was favorable for the maintenance of HNV at the LLHNV. It should be noted that, around 1800 UTC 06 October, there was an intense positive center of baroclinic conversion which was mainly located between 700 and 400 hPa. Supported by the favorable baroclinic conversion, the HNV stretched to 500 hPa during this period (Fig. 2g). However, after 0000 UTC 07 October, the baroclinic conversion became intensely negative, and the top level of HNV lowered. During the MS, especially the initiation stage of the HNV, the horizontal advection of EKE by background circulations (term K3) was very favorable for the development of HNV at the LT. The vertical advection of EKE by the background circulations (term K4) was also very favorable for the vertical stretching of HNV at the MT. During the DS, both advection terms weakened significantly with nearly the same influences on HNV: before 0000 UTC 09 October, terms K3 and K4 were mainly favorable for the maintenance of HNV; after that, they mainly served as sinks of the EKE, thereby accelerating the attenuation of the HNV. During the MS, especially the initiation of HNV, the horizontal and vertical eddy fluxes of eddy geopotential energy (terms K5 and K6) remained positive at the LLHNV, which indicates the interactions between HNV and other synoptic systems were favorable for the formation and maintenance of HNV, while at the HLHNV, terms K5 and K6 mainly transported eddy geopotential energy out of the KA, which reduced the EKE of the HNV. During the DS, before the dissipation, term K5 mainly enhanced EKE while term K6 mainly reduced the EKE; however, around the dissipation, their effects reversed.

Six hours before the formation of HNV, the barotropic energy conversion and vertical advection by background circulations (term K4) dominated the formation of HNV at the HLHNV (Fig. 7c), while the positive vertical eddy flux of eddy geopotential energy (term K6) which was associated with convective activities dominated the formation at the LLHNV. Six hours before the dissipation of HNV, the horizontal and vertical eddy fluxes of eddy potential energy (terms K5 and K6) were main sinks of EKE at the HLHNV (Fig. 7d), while the horizontal and vertical fluxes of EKE by back ground circulations dominated the dissipation of EKE at the LLHNV.

During the MS, the vertical advection by background circulations was the most favorable factor for the maintenance of EKE at the HLHNV (Fig. 8c), while the horizontal advection by background circulations and vertical eddy flux of eddy geopotential energy were the dominant factors for the maintenance of the HNV at the LLHNV. During the DS, the intensity of all the EKE budget terms decreased remarkably (Fig. 8d); the horizontal eddy flux of eddy potential energy and vertical advection by background circulations dominated the maintenance of EKE. The baroclinic energy conversion and vertical eddy flux of eddy potential energy dominated the decreasing processes of EKE at the HLHNV and LLHNV, respectively.

4.3 Budgets of vertical helicity

Lilly (1986) found that the effects of helicity seemed to be dominant in long-lived storms, because the helicity may reduce the energy loss and resist dissipation. Thus the vertical helicity budget was calculated with Eq. 3 to investigate the variation of helicity which was essential to the maintaining of HNV. As shown in Fig. 10a, during the lifetime of the HNV, there was an intense positive helicity zone below 5,500 m which was associated with the HNV. The helicity reached maximum around 2,000 m when the HNV formed and then weakened with time as the positive vorticity decreased (Fig. 6a). Helicity during the MS was more intense than that of DS and so did all the budget terms of the vertical helicity equations. In the DS, helicity mainly remained positive which was favorable for the maintenance of HNV; however, around the dissipation of HNV the helicity decreased significantly.

During the MS, horizontal helicity mainly converted to vertical helicity (Fig. 10b) and therefore enhanced the vertical helicity, whereas during the DS, term CON remained mainly negative, indicating that the vertical helicity converted to horizontal one. From Fig. 10c, d, the horizontal and vertical advections of helicity both transported helicity out of the KA at the LLHNV, which contributed to the decrease of helicity there. However, at the HLHNV, both advection terms mainly remained positive, which were favorable for the increase of helicity. At the LLHNV, term Z1 mainly remained positive (Fig. 10e), which indicates that buoyancy was very important for the increase of helicity, whereas at the HLHNV, term Z1 mainly remained negative, which decreased the helicity. Term Z4 mainly remained positive at the LLHNV (Fig. 10f), corresponding to the intense convergence there (Fig. 6a), and this was favorable for the maintenance of positive helicity. However, at the HLHNV, term Z4 mainly acted as a sink of helicity, corresponding to the divergence there. The vertical solenoid (term Z2) only had slightly negative effects on the helicity, since it was two orders
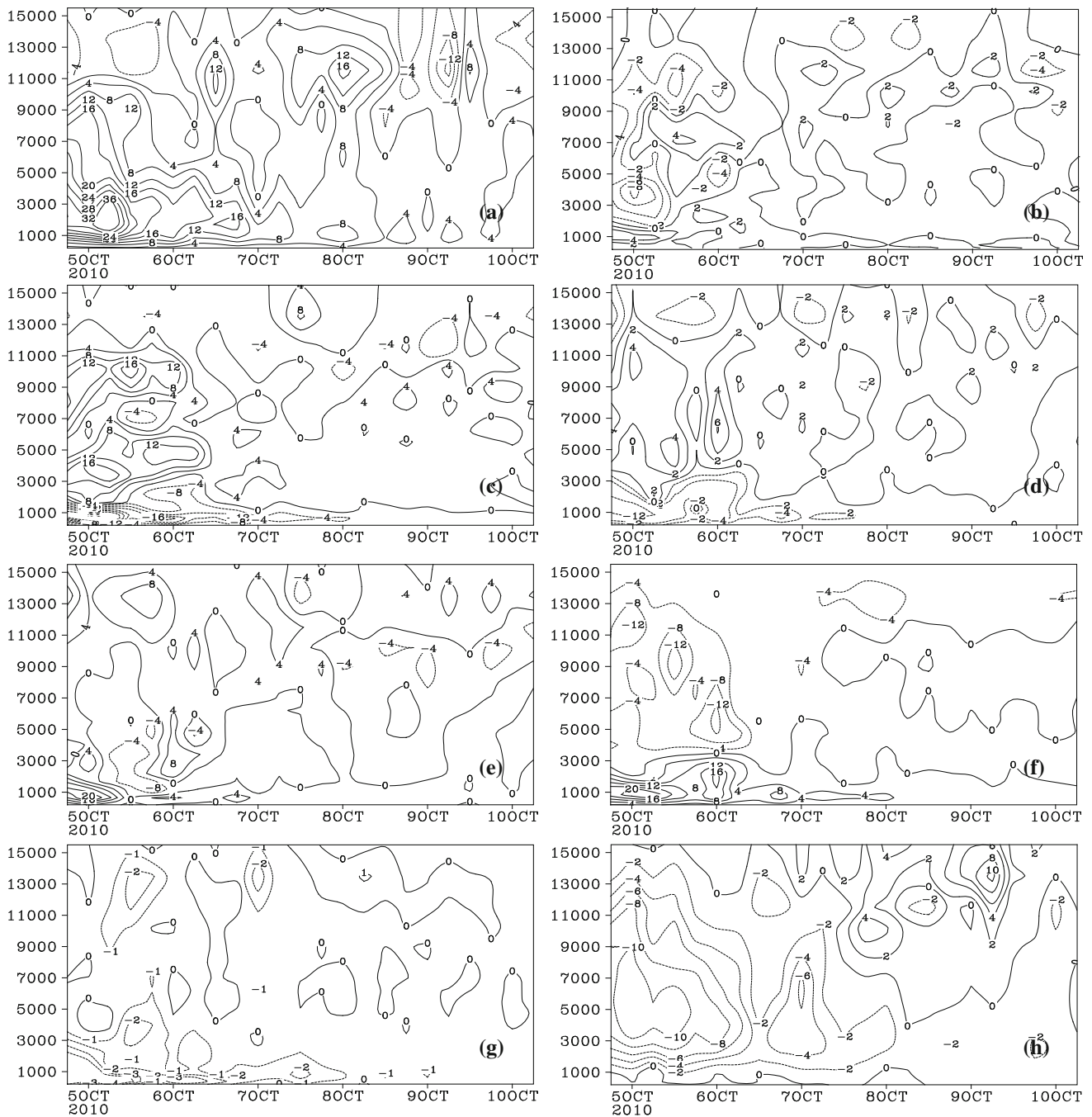
Fig. 10 Cross sections of vertical helicity and budgets of the helicity equation. **a** distribution of vertical helicity (10^{-7} m s^{-2}), **b** term CON (10^{-11} m s^{-3}), **c** vertical helicity advection (10^{-11} m s^{-3}), **d** horizontal helicity advection (10^{-11} m s^{-3}), **e** term Z1 (10^{-11} m s^{-3}), **f** term Z4 (10^{-11} m s^{-3}), **g** term Z2 (10^{-13} m s^{-3}), and **h** term Z3 (10^{-12} m s^{-3})

smaller than the main terms of the helicity budget equation. Term Z3 mainly decreased the helicity; however, since β is very small, this term is one order smaller than other main terms. From the above, at the LLHNV, the maintenance of helicity mainly relied on the buoyancy and convergence (terms Z1 and Z4), while at higher levels of the HNV, the horizontal and vertical advections were the dominant factors.

5 Summary and conclusions

During the period of 0600 UTC, 05 October 2010–1800 UTC 09 October, a mesoscale vortex occurred over Hainan and caused several heavy rainfall episodes, with the maximum 3-h precipitation of up to 70 mm (Fig. 4). The HNV was mainly located below 500 hPa, with a tropical depression over Hainan.

During the lifetime of the HNV, activities of easterly wave was not obvious; thus the HNV was different from the typical vortices associated with the easterly wave which were mainly dominated by tilting and convergence (Arnault and Roux 2010). The budgets of vorticity, EKE, and vertical helicity were calculated to study the formation, maintenance, dissipation of the HNV, as well as the interactions between the HNV, and background circulations. The main results are as follows:

(a) The HNV varied in different way among different levels; thus the vertical stretching of HNV was divided into two parts, namely the HLHNV and LLHNV. Intense convergence dominated the formation at the LLHNV, while the vertical transport of positive vorticity which is associated with the intense convective activities dominated the formation at the HLHNV. Based on the variations of the HNV (stream field, vorticity and ascending motions), the lifetime of HNV was divided into the MS and DS. During the MS, the HNV remained intense. The positive horizontal and vertical vorticity advections were the most important factors for the maintenance of HNV at the HLHNV, while intense convergence was the most favorable factor for the maintenance of the HNV at the LLHNV. During the period of DS, the HNV significantly weakened gradually. The convergence and positive vertical vorticity advection associated with convective activities were the most important factors which resisted the decaying of the HNV. In addition, the divergence and the conversion from vertical vorticity to horizontal one dominated the attenuation of the HNV at the HLHNV and LLHNV, respectively. The horizontal transport of positive vorticity out of the KA and the conversion from vertical vorticity to horizontal one caused the dissipation of HNV directly.

(b) During the lifetime of HNV, there were obvious interactions between the HNV and background circulations, as well as interactions between the HNV and other synoptic systems, both of which were very important to the variations of the HNV. Barotropic energy conversion was very important for the formation of HNV, while baroclinic energy conversion dominated the decaying process at the HLHNV during the DS. The above results are different from Ding and Liu (1985), since in their case, the baroclinic energy conversion was conducive to the maintenance of a typhoon, while the barotropic energy conversion was detrimental to the typhoon. In addition, for our case, the baroclinic energy conversion may be closely related to the variation of the vertical stretching of the vortex. Transports by the background circulations were very important for the formation and maintenance of HNV, while around its dissipation, they became the main sinks of EKE at the LLHNV. Interactions between the HNV and other synoptic systems were mainly favorable for the formation and maintenance of HNV at the LLHNV. However, at the HLHNV, the interactions mainly

Table 1 The dominant factors favorable for the formation and longevity of the HNV

	High levels of the HNV (HLHNV)	Low levels of the HNV (LLHNV)
Formation	Term V2	Term V5
	Terms K1 and K4	Term K6
Maintaining stage (MS)	Terms V1 and V2	Term V5
	Term K4	Terms K3 and K6
Decaying stage (DS)	Term V2	Terms V2 and V5
	Terms K4 and K5	Term K5

Table 2 The factors dominating the decaying process and dissipation of HNV

	High levels of the HNV (HLHNV)	Low levels of the HNV (LLHNV)
Decaying stage (DS)	Term V5	Term V3
	Term K2	Term K6
Dissipation	Term V1	Terms V1 and V3
	Terms K5 and K6	Terms K3 and K4

served as sinks of the EKE. The dominant factors in different stages of the HNV among different levels are summarized and listed in Tables 1 and 2.

(c) For the duration of the HNV, there was no remarkable frequency dispersion, which was very favorable for the long-time maintenance of HNV. Among the levels of HNV, helicity remained positive, which could reduce the energy loss and resist dissipation, and thus this was another favorable condition for the longevity of HNV. The variations of helicity which is closely related to the HNV, was determined by factors as follows: during the MS, horizontal helicity mainly converted to vertical helicity which enhanced the vertical helicity, whereas in the DS, term CON acted conversely. At the LLHNV, the buoyancy and convergence were the most favorable factors for the maintenance of positive helicity, while at the HLHNV, horizontal and vertical advections of helicity were the dominant effects.

References

Akiyama T (1984) A medium-scale cloud cluster in a Baiu front. Part I: evolution process and fine structure. J Meteorol Soc Jpn 62:485–504

Arnault J, Roux F (2010) Comparison between two case studies of developing and nondeveloping African easterly waves during NAMMA and AMMA/SOP-3: absolute vertical vorticity budget. Mon Wea Rev 138:1420–1445

Bartels DL, Maddox RA (1991) Midlevel cyclonic vortices generated by mesoscale convective systems. Mon Wea Rev 119:104–117

Chen S-J, Lorenzo D (1984) Numerical prediction of the heavy rain vortex over eastern Asia monsoon region. J Meteor Soc Japan 62:730–747

Davis CA, Galarneau TJ (2009) The vertical structure of mesoscale convective vortices. J Atmos Sci 66:686–704

Ding Y-H, Liu Y-Z (1985) On the analysis of typhoon kinetic energy. Part I. Budget of total kinetic energy and eddy kinetic energy. Sci China (B) 15:957–966 (in Chinese)

Fu S-M, Sun J-H, Zhao S-X, Li W-L (2009) An analysis of the eddy kinetic energy budget of a southwest vortex during heavy rainfall over south China. Atmos Ocean Sci Lett 2:135–141

Fu S-M, Sun J-H, Zhao S-X (2011a) On the significance and use of the horizontal and vertical helicity budget equations. Geophys Res Lett (submitted)

Fu S-M, Sun J-H, Zhao S-X, Li W-L (2011b) The energy budget of a southwest vortex with heavy rainfall over south China. Adv Atmos Sci 28:709–724

Hendricks EA, Montgomery MT, Davis CA (2004) The role of "vortical" hot towers in the formation of tropical cyclone Diana (1984). J Atmos Sci 61:1209–1232

Johnston EC (1982) Mesoscale vorticity centers induced by meso-scale convective complexes. In: Ninth conf. on weather forecasting and analysis. Amer Meteor Soc, Seattle, WA, pp 196–200 (preprints)

Joyce RJ, Janowiak JE, Arkin PA, Xie P (2004) CMORPH: a method that produces global precipitation estimates from passive microwave and infrared data at high spatial and temporal resolution. J Hydrometeor 5:487–503

Kirk JR (2007) A phase-plot method for diagnosing vorticity concentration mechanisms in mesoscale convective vortices. Mon Wea Rev 135:801–820

Knievel JC, Johnson RH (2002) The kinematics of a midlatitude, continental mesoscale convective system and its mesoscale vortex. Mon Wea Rev 130:1749–1770

Lilly DK (1986) The structure, energetics and propagation of rotating convective storms. Part II: helicity and storm stabilization. J Atmos Sci 43:126–140

Lu H-C, Chen W, Zhu M, Song X-L, Kang J-W (2002) Mechanism study of meso-β scale vortex system of heavy rain in Meiyu front. J PLA Univ Sci Technol 3:70–76 (in Chinese)

Montgomery MT, Nicholis ME, Cram TA, Saunder AB (2006) A vortical hot tower route to tropical cyclogenesis. J Atmos Sci 63:355–386

Ni Y-Q, Zhou X-J (2006) Study on formation mechanisms of heavy rainfall within the Meiyu along the mid-lower Yangtze River and theories and methods of their detection and prediction. Acta Meteorologica Sincia 20:191–208

Ninomiya K (2000) Large and meso-α scale characteristics of Meiyu/Baiu front associated with intense rainfalls in 1–10 July 1991. J Meteorol Soc Japan 78:141–157

Shen X-Y, Ni Y-Q, Zhang M, Zhao N, Peng L-X (2005) A possible mechanism of the genesis and development of meso-β rainstorm system part I: phase velocity of vortex Rossby waves. Chin J Atmos Sci 29:727–733 (in Chinese)

Simpson JE, Ritchie E, Holland GJ, Halverson J, Stewart S (1997) Mesoscale interactions in tropical cyclone genesis. Mon Wea Rev l25:2643–2661

Tao S-Y (1980) Rainstorms in China. Science Press, Beijing (in Chinese)

Tirer SB, Davis CA (2002) Influence of balanced motion on heavy precipitation within a long-lived convectively generated vortex. Mon Wea Rev 130:877–899

Zhang D-L, Ban N (1996) Oceanic cyclogenesis as induced by a mesoscale convective system moving offshore. Part II: genesis and thermodynamic transformation. Mon Wea Rev l24:2206–2226

Zhao S-X, Tao Z-Y, Sun J-H (2004) Study on mechanism of heavy rainfall on Meiyu (Baiu) front in Yangtze River Valley. China Meteorological Press, Beijing (in Chinese)

Zhou H-G, Wang Y-B (2005) Structure of meso-β and -γ scale on Meiyu in Huaihe River Basin on 30 June, 2003 by dual-Doppler Radar. Acta Meteorologica Sincia 63:301–312 (in Chinese)